Supporting Information

Chemoselective and Living/Controlled Polymerization of Polar Divinyl Monomers by *N*-Heterocyclic Olefin Based Classical and Frustrated Lewis Pairs

Wuchao Zhao, *Qianyi Wang*, Jianghua He and Yuetao Zhang*

State Key Laboratory of Supramolecular Structure and Materials, College of Chemistry, Jilin University, Changchun, Jilin 130012, China.

* Corresponding author. E-mails: ytzhang2009@jlu.edu.cn

Table of Contents

1. Preparation of NHO1-3 and Al-based Lewis acid

Tris(pentafluorophenyl)borane, $B(C_6F_5)_3$, was prepared according to literature procedures.[1] $Al(C_6F_5)_3$, as a $(toluene)_{0.5}$ adduct, or in its unsolvated form, was prepared by ligand exchange reactions between $B(C_6F_5)_3$ and $AlMe_3$ or $AlEt_3$ (for preparation of the unsolvated form)[2] (Extra caution should be exercised when handling these materials, especially the unsolvated $Al(C_6F_5)_3$, due to its thermal and shock sensitivity!). Literature procedures were employed for the preparation of the following compounds: 2-isopropyl-4-methyl-1*H*-imidazole,[3] 2-isopropyl-5-methyl-4-phenyl-1*H*- imidazole,[3,4] 1,3-Dimethyl- 4,5- diphenyl-2-(propan-2-ylidene)-2,3- dihydro-1*H*-imidazole (**NHO1**),[5] and methyl bis(2,6-di-^{t}Bu-4- methylphenoxy)aluminum ($MeAl(BHT)_2$),[6] 1,3,4-trimethyl-5-phenyl-2- (propan-2-ylidene)-2,3-dihydro-1*H*-imidazole (**NHO2**), 1,3,4-trimethyl-2- (propan-2-ylidene)-2,3-dihydro-1*H*-imidazole (**NHO3**).[8]

2. Synthesis of NHO4-7

NHO4-7 were synthesized according to following procedures[7,8]:

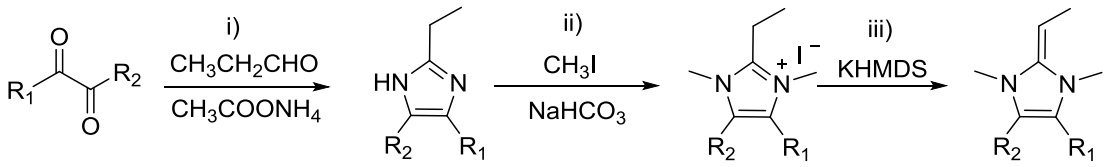

Scheme S1: preparation procedures of **NHO4-7**

NMR spectrum data:

2-ethyl-1,3-dimethyl-4,5-diphenyl-1*H*-imidazol-3-ium iodide: ^{1}H NMR (500 MHz, $CDCl_3$) δ 7.42-7.35 (m, 10H, *Ph*), 3.75 (s, 6H, NCH_3), 3.36 (q, *J* = 8 Hz, 4H, CH_2), 1.47 (t, *J* = 8 Hz, 3H, CH_2CH_3).

2-ethylidene-1,3-dimethyl-4,5-diphenyl-2,3-dihydro-1*H*-imidazole (NHO4): ^{1}H NMR (500 MHz, Benzene-d_6) δ 7.19- 6.90 (m, 10H, *Ph*), 3.36 (q, *J* = 5 Hz, 1H, CH_3CH), 2.96 (s, 3H, NCH_3), 2.56 (s, 3H, NCH_3), 2.12 (d, *J* = 5 Hz, 3H, CH_3CH). ^{13}C NMR (126 MHz, Benzene-d_6) δ 153.2, 131.49, 131.0, 129.8, 128.4, 128.4, 128.3, 127.1, 127.0, 125.9, 125.7, 59.6, 37.2, 31.6, 12.2.

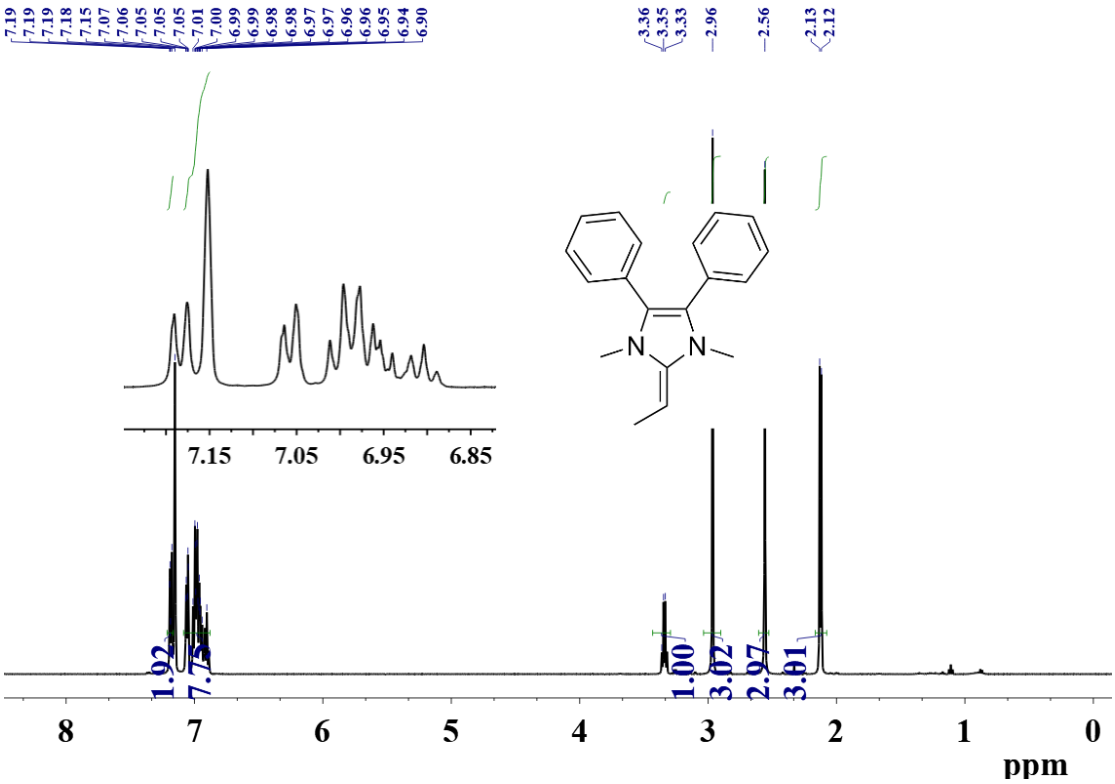

Fig S1. ^{1}H NMR spectrum of **NHO4** (Benzene-d_6, 500 MHz).

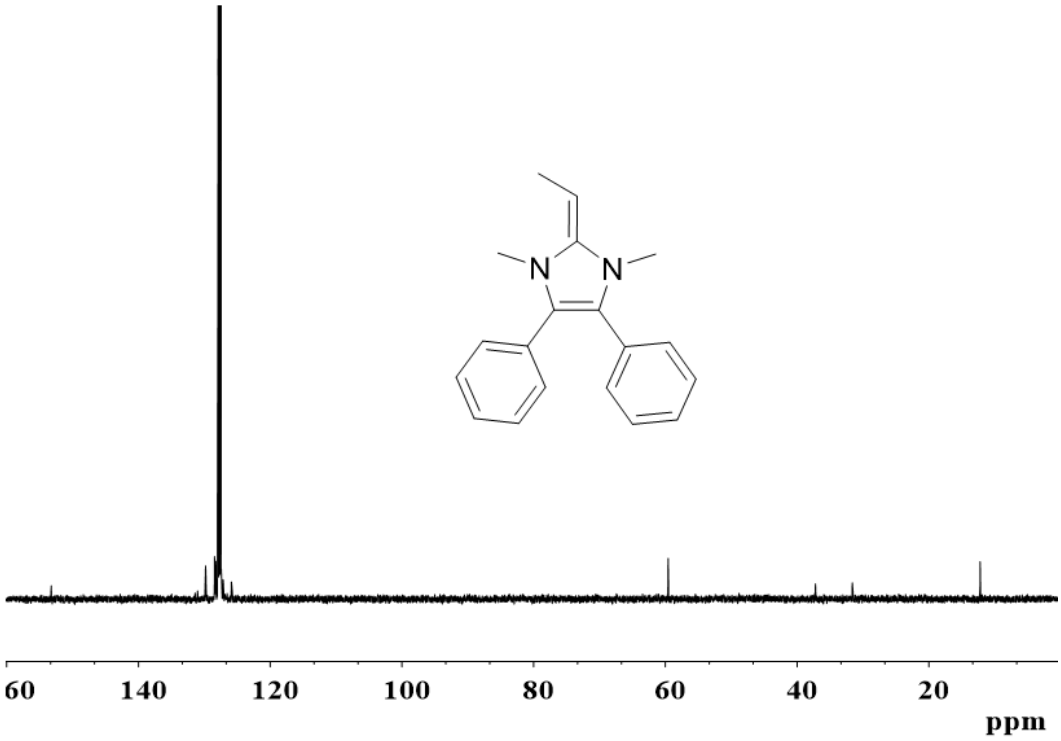

Fig S2. ^{13}C NMR spectrum of **NHO4** (Benzene-d_6, 126 MHz).

2-ethyl-1,3,5-trimethyl-4-phenyl-1H-imidazol-3-ium iodide: ^{1}H NMR (500 MHz, $CDCl_3$) δ 7.57-7.50 (m, 3H, *Ph*), 7.50-7.42 (m, 2H, *Ph)*, 3.88 (3H, NCH_3), 3.67 (3H, NCH_3), 3.31 (q, *J* = 10 Hz, 2H, CH_2), 2.28 (s, 3H, CH_2CH_3), 1.41 (t, *J* = 10 Hz, 3H, CCH_3).

2-ethylidene-1,3,4-trimethyl-5-phenyl-2,3-dihydro-1*H*-imidazole (NHO5): ^{1}H NMR (500 MHz, C_6D6) δ 7.27-7.01 (m, 5H, *Ph*), 3.25-3.20 (q, *J* = 5 Hz, 1H, CH_3CH), 2.93-2.92 (3H, NCH_3), 2.63-2.44 (3H, NCH_3), 2.20-2.12 (d, *J* = 5 Hz, 3H, CH_3CH), 1.61-1.55 (3H, CCH_3). ^{13}C NMR (126 MHz, C_6D_6) δ 152.6, 151.2, 132.4, 131.8, 128.8, 128.4, 128.3, 126.2, 125.3, 123.6, 123.5, 121.3, 119.3, 58.7, 55.9, 37.4, 32.6, 32.5, 28.8, 12.2, 11.8, 9.4, 9.2.

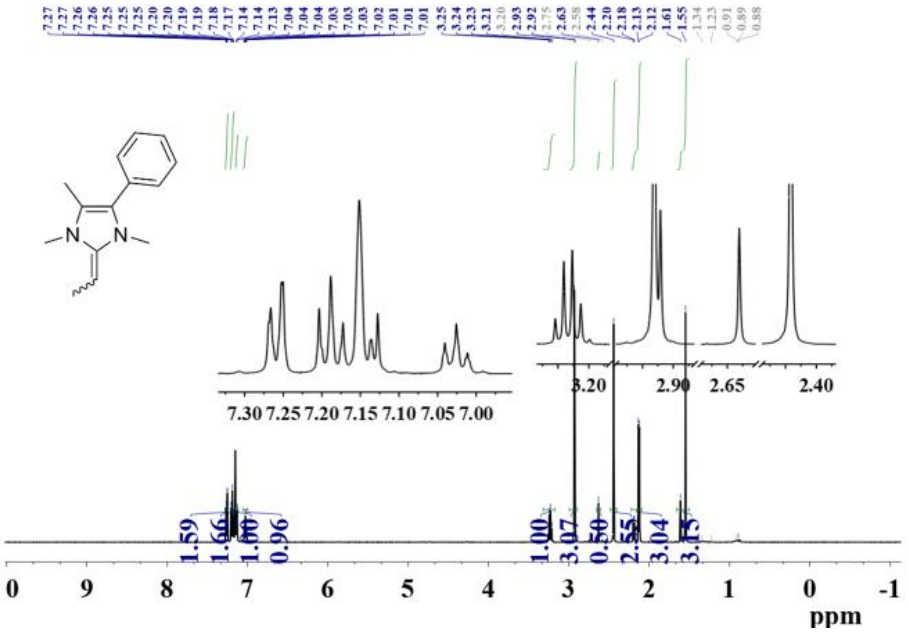

Fig S3. ^{1}H NMR spectrum of **NHO5** (Benzene-d_6, 500 MHz).

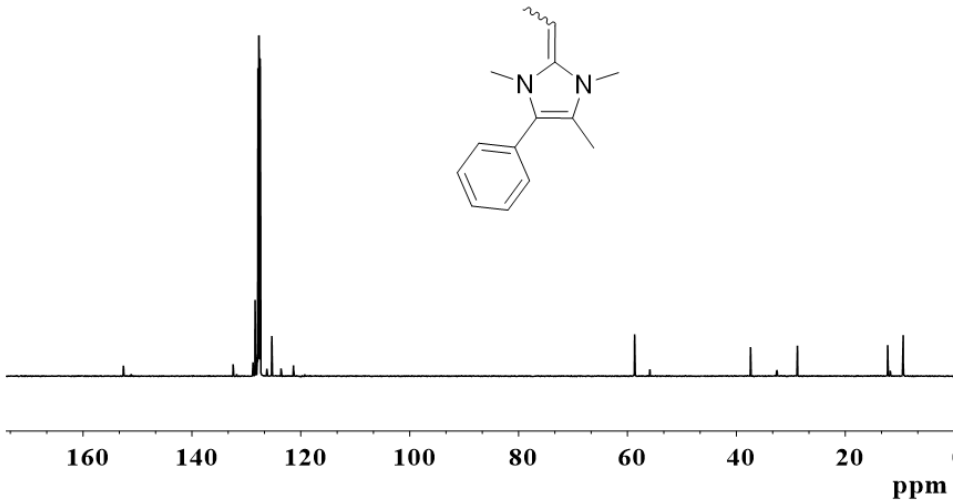

Fig S4. ^{13}C NMR spectrum of **NHO5** (Benzene-d_6, 126 MHz).

2-ethylidene-1,3,4-trimethyl-2,3-dihydro-1*H*-imidazole (NHO6): ^{1}H NMR (500 MHz, C_6D6) δ 5.21-5.15 (1H, CH_3CCH), 3.08-2.90 (m, 1H, CH_3CH), 2.87-2.89 (3H, NCH_3), 2.48-2.42 (3H, NCH_3), 2.17-2.14 (d, J = 7 Hz, 3H, CH_3CH), 1.54-1.46 (3H, CH_3C). ^{13}C NMR (126 MHz, C_6D6) δ 150.6, 121.0, 119.7, 111.6, 111.4, 55.1, 53.9, 36.5, 32.7, 32.4, 28.7, 11.7, 11.6, 9.7, 9.4.

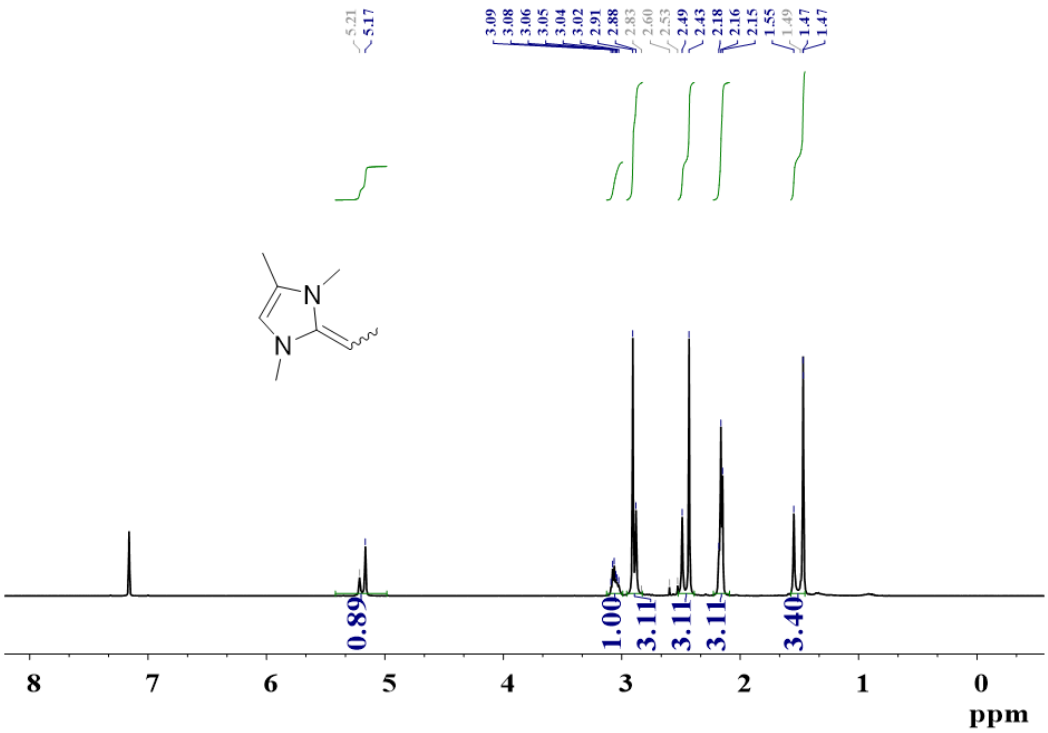

Fig S5. ^{1}H NMR spectrum of **NHO6** (Benzene-d_6, 500 MHz).

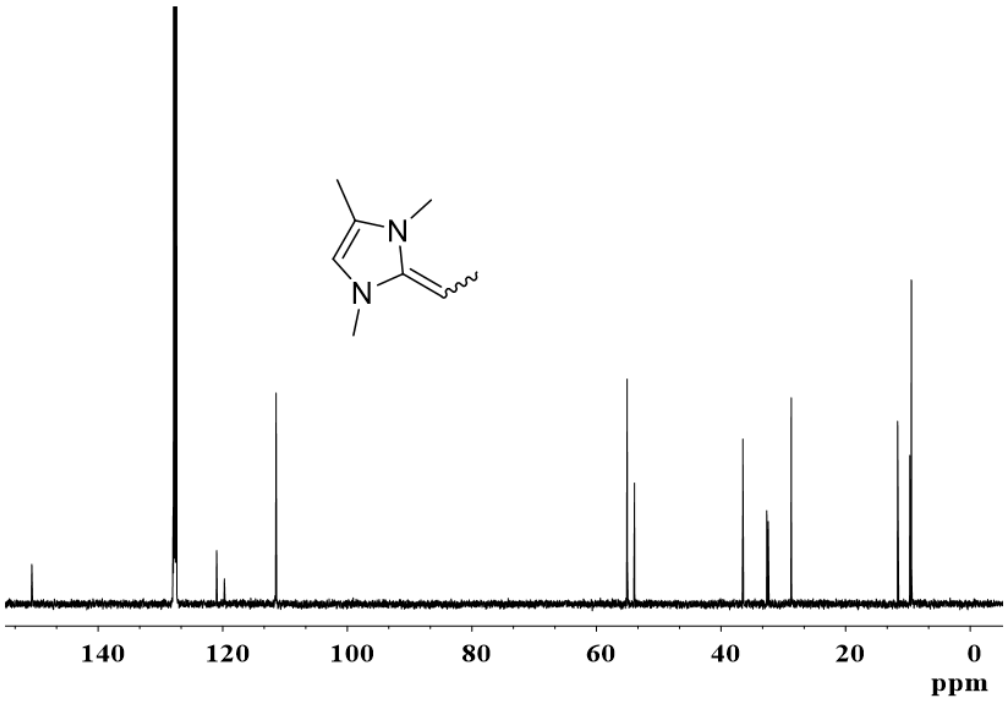

Fig S6. ^{13}C NMR spectrum of **NHO6** (Benzene-d_6,126 MHz)

1,2,3,4-tetramethyl-1H-imidazol-3-ium iodide: ^{1}H NMR (500 MHz, $CDCl_3$) δ 7.22 (m, 1H, C*H*), 3.85 (3H, NCH_3), 3.72 (3H, NCH_3), 2.28 (3H, CH_3), 2.27(3H, CCH_3).

1,3,4-trimethyl-2-methylene-2,3-dihydro-1*H*-imidazole (NHO7): ^{1}H NMR (500 MHz, C_6D_6) δ5.24 (s, 1H, C*H*), 2.82 (d, *J* = 15, 2H, CH_2), 2.59 (3H, NCH_3), 2.53 (3H, NCH_3), 1.48 (3H, CCH_3). ^{13}C NMR (126 MHz, C_6D_6) δ 153.5, 119.1, 109.4, 40.1, 32.1, 28.6, 9.2.

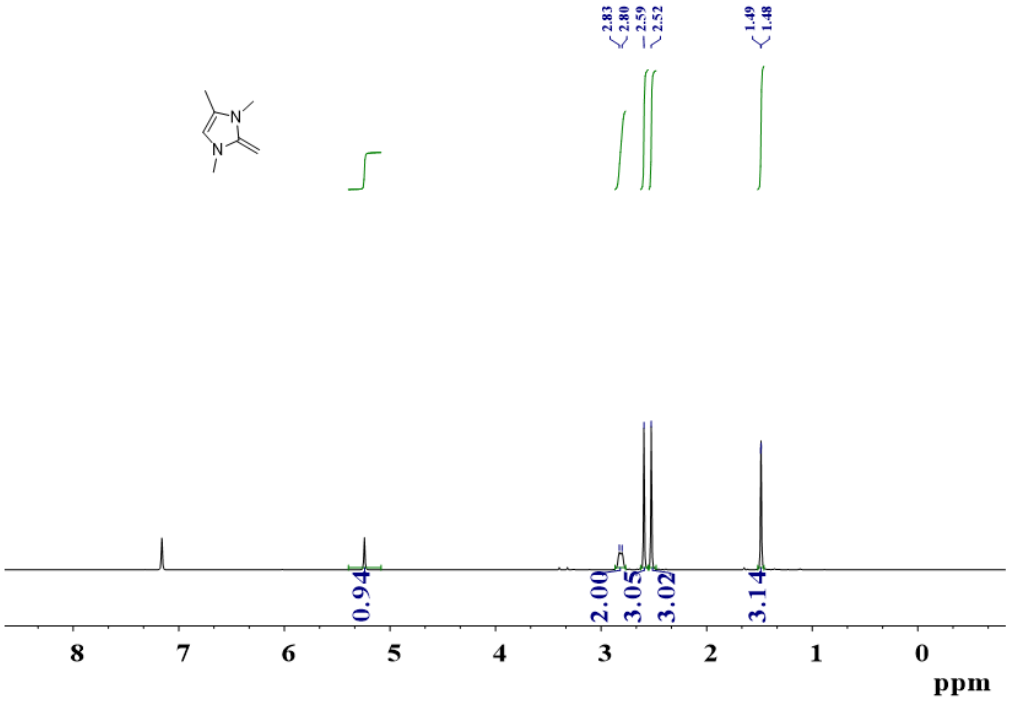

Fig S7. ^{1}H NMR spectrum of **NHO7** (Benzene-d_6, 500 MHz).

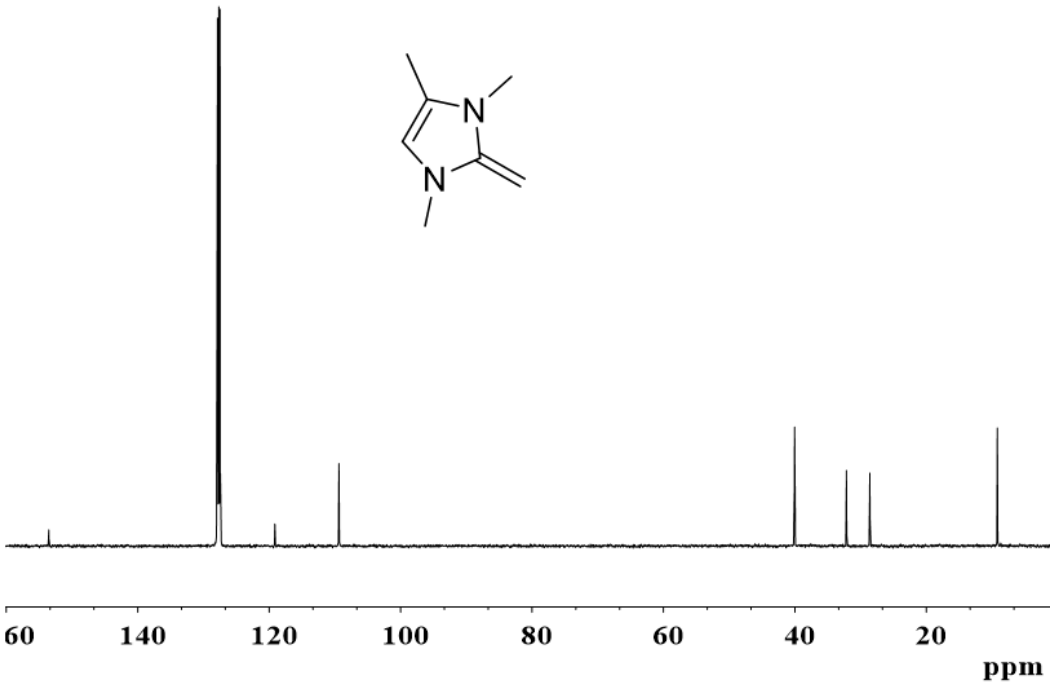

Fig S8. ^{13}C NMR spectrum of **NHO7** (Benzene-d_6, 126 MHz)

3. NMR reaction of NHO4 with MeAl(BHT)2

A Teflon-valve-sealed J. Young-type NMR tube was charged with **NHO4** (5.5 mg, 0.02 mmol) and 0.3 mL of C_6D_6. A solution of $MeAl(BHT)_2$ (9.6 mg, 0.02 mmol in 0.3 mL C_6D_6) was added to this tube via pipette at ambient temperature, and the mixture was allowed to react for 15 min before analysis by NMR, which showed no reaction between Lewis acid and Lewis base.

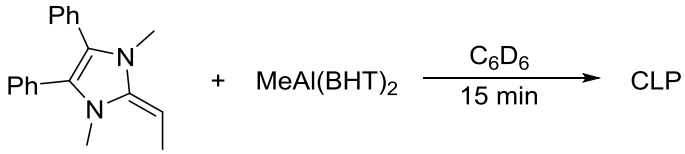

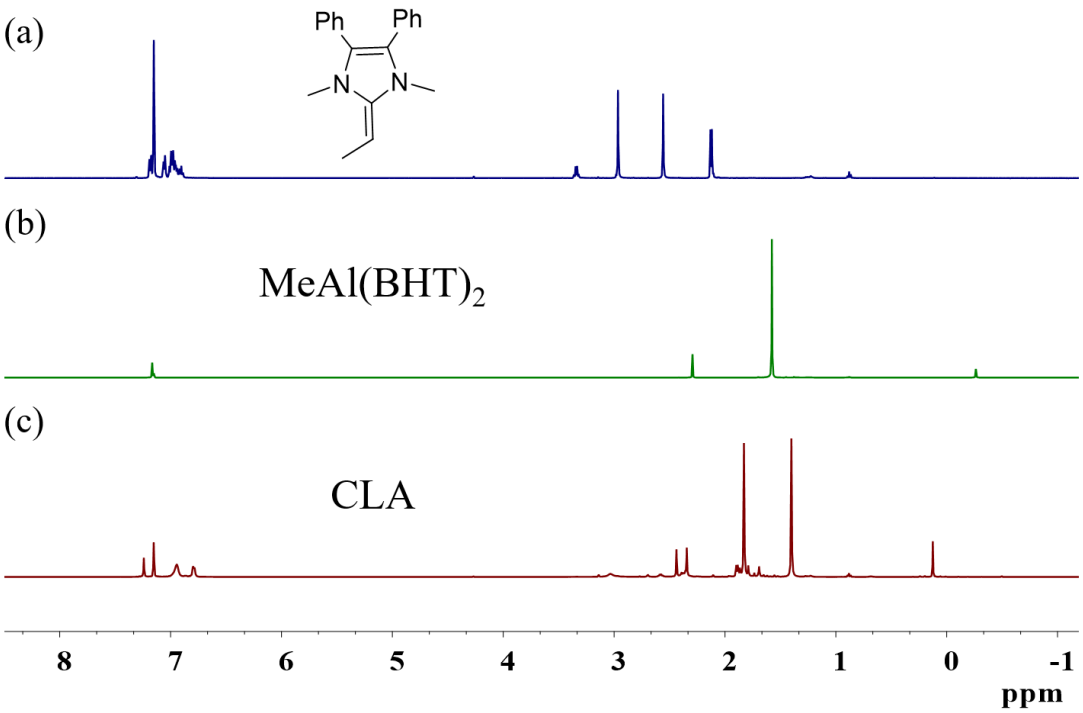

Fig S9. Overlay of ^{1}H NMR spectra for: (a) **NHO4**, (b) MeAl(BHT)$_2$, and (c) CLA generated from the reaction of MeAl(BHT)$_2$ with MeAl(BHT)$_2$ (Benzene-d_6, 500 MHz)

4. NMR reaction of NHO4-6 with MeAl(BHT)$_2$·MMA

General procedure: A Teflon-valve-sealed J. Young-type NMR tube was charged with NHO (0.02 mmol) and 0.3 mL of C_6D_6. A solution of MeAl(BHT)$_2$·MMA (11.6 mg, 0.02 mmol, 0.3 mL C_6D_6) was added to this tube via pipette at ambient temperature, and the mixture was allowed to react for 15 min before analysis by ^{1}H NMR, which showed generates zwitterionic enolaluminate.

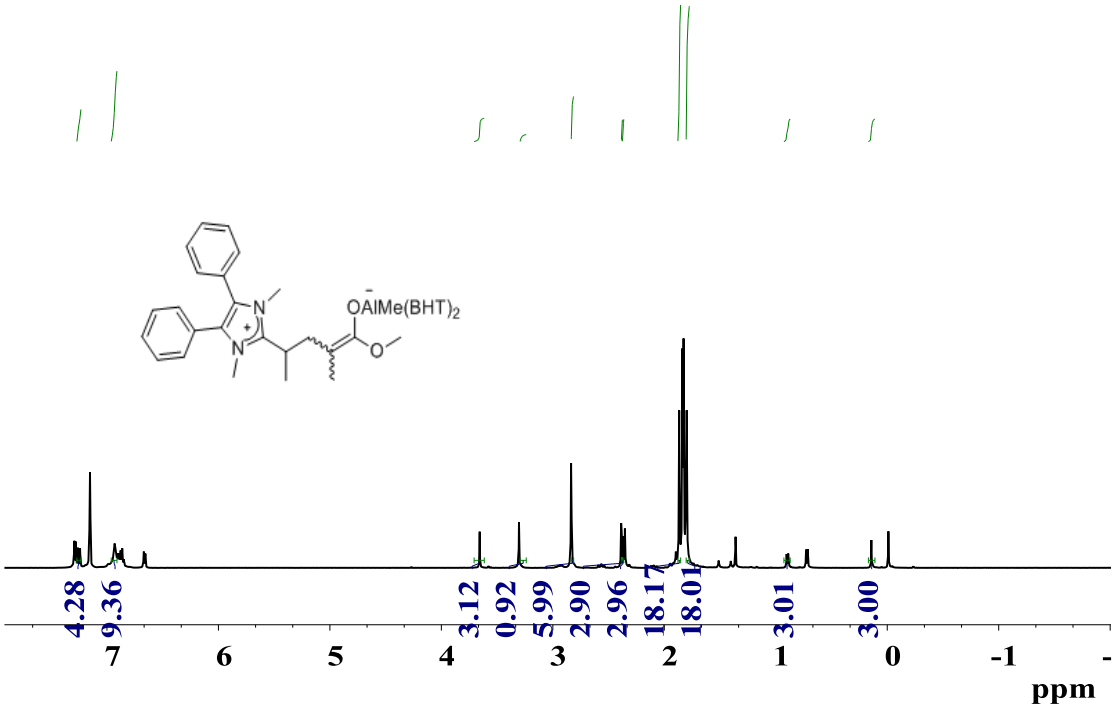

Fig S10 ^{1}H NMR spectrum (benzene-d_6, 500 MHz) of the reaction with **NHO4**/ MeAl(BHT)$_2$·MMA = 1:1 ratio at RT (we only mark the zwitterionic enolaluminate).

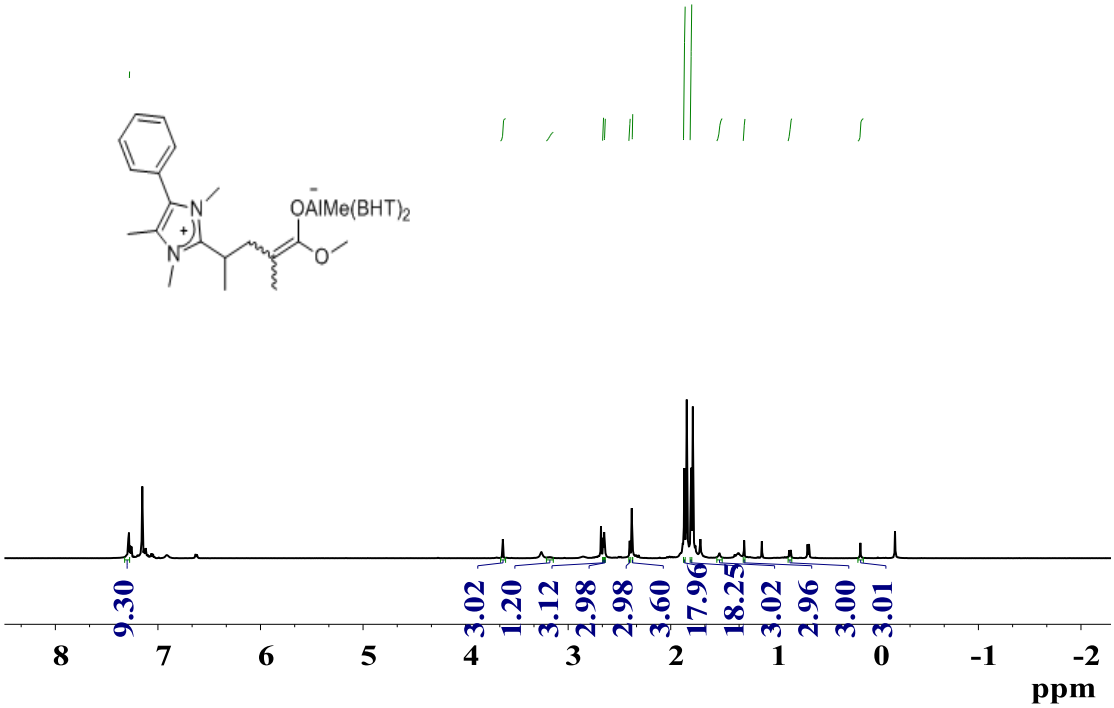

Fig S11 ^{1}H NMR spectrum (benzene-d_6, 500 MHz) of the reaction with **NHO5**/ MeAl(BHT)$_2$·MMA = 1:1 ratio at RT (we only mark the zwitterionic enolaluminate).

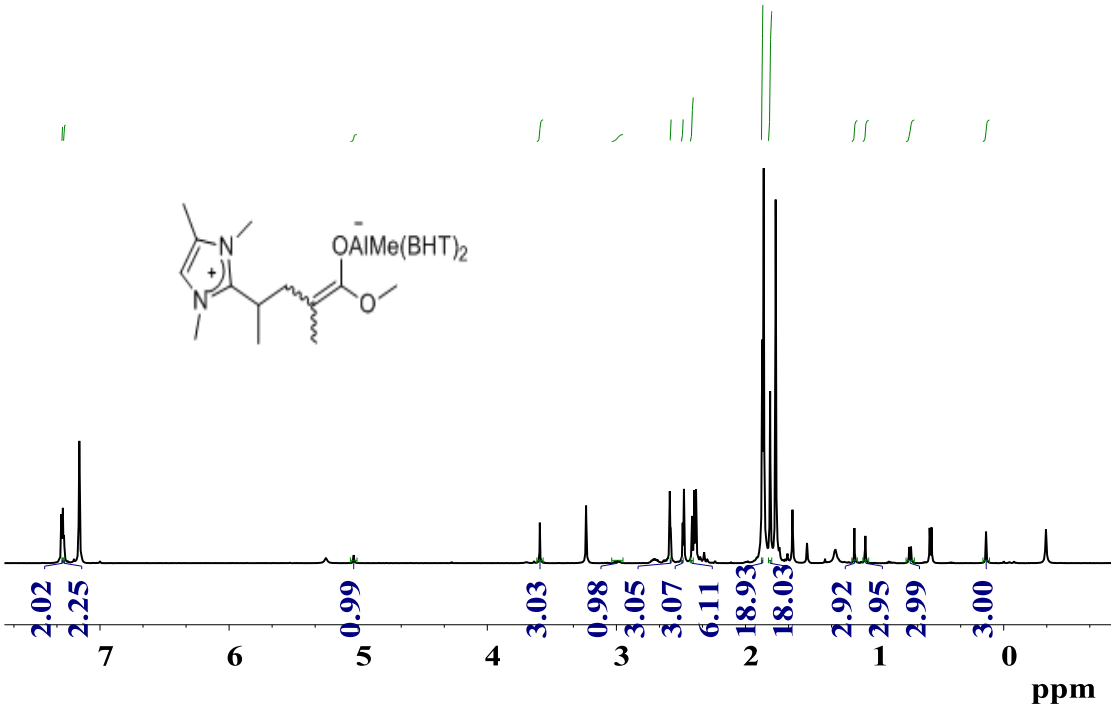

Fig S12 ^{1}H NMR spectrum (benzene-d_6, 500 MHz) of the reaction with **NHO6**/ MeAl(BHT)$_2$·MMA = 1:1 ratio at RT (we only mark the zwitterionic enolaluminate)

5. Synthesis and isolation of INT

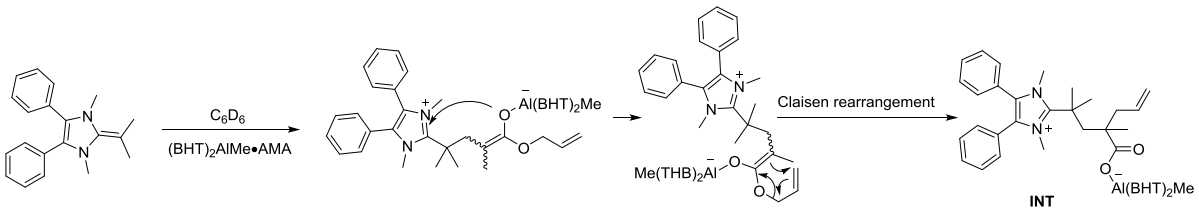

Scheme S2. Stoichiometric reaction of **NHO1** with MeAl(BHT)$_2$·AMA = 1:1 ratio at RT

A 20 mL glass vial was charged with **NHO1** (120.0 mg) and 5 mL of toluene, while another vial was charged with MeAl(BHT)$_2$·AMA (251.0 mg) and 50 mL of hexane. The two vials were mixed via pipet at ambient temperature to give a light-yellow suspension. The solid was collected by filtration, then washed with hexane and dried *in vacuo* (238.0 mg, 64%). ^{1}H NMR (dichloromethane-d_2, 500 MHz) δ 7.52-7.44 (m, 6H,

Ph) 7.26-7.24 (m, 4H, *Ph*) 6.93 (s, 2H, BHT-*Ph*), 6.85 (s, 2H, BHT-*Ph*) 5.85-5.80 (m, 1H, *CH*CH_2), 5.13-5.08 (m, 2H, *CHCH*$_2$), 3.74 (s, 6H, NCH_3), 2.54 (d, *J* = 15, 1H, Me_2CCH_2), 2.47-2.32 (M, 2H, =CHCH_2), 2.21 (s, 3H, Ar-CH_3), 2.18 (s, 3H, Ar-CH_3), 2.04 (d, 1H, *J* = 15, 1H, Me_2CCH_2), 1.78 (s, 3H, *Me*$_2$C), 1.77 (s, 3H, *Me*$_2$C), 1.44 (s, 36H,*tBu*), 1.17 (s, 3H, *Me*CCO_2), -0.55 (s, 3H, Al*Me*). ^{13}C NMR (126 MHz, Benzene-d_6) δ 157.3, 156.9, 151.7, 138.7, 131.4, 130.5, 130.3, 129.3, 129.2, 125.6, 125.5, 122.7, 74.4, 54.6, 44.0, 41.7, 35.9, 35.4, 34.5, 32.2, 29.2, 21.3, 15.6, 9.0. Due to the poor solubility of **INT** in C_6D_6 and instability in CD_2Cl_2, pure ^{13}C NMR spectrum was unable obtained.

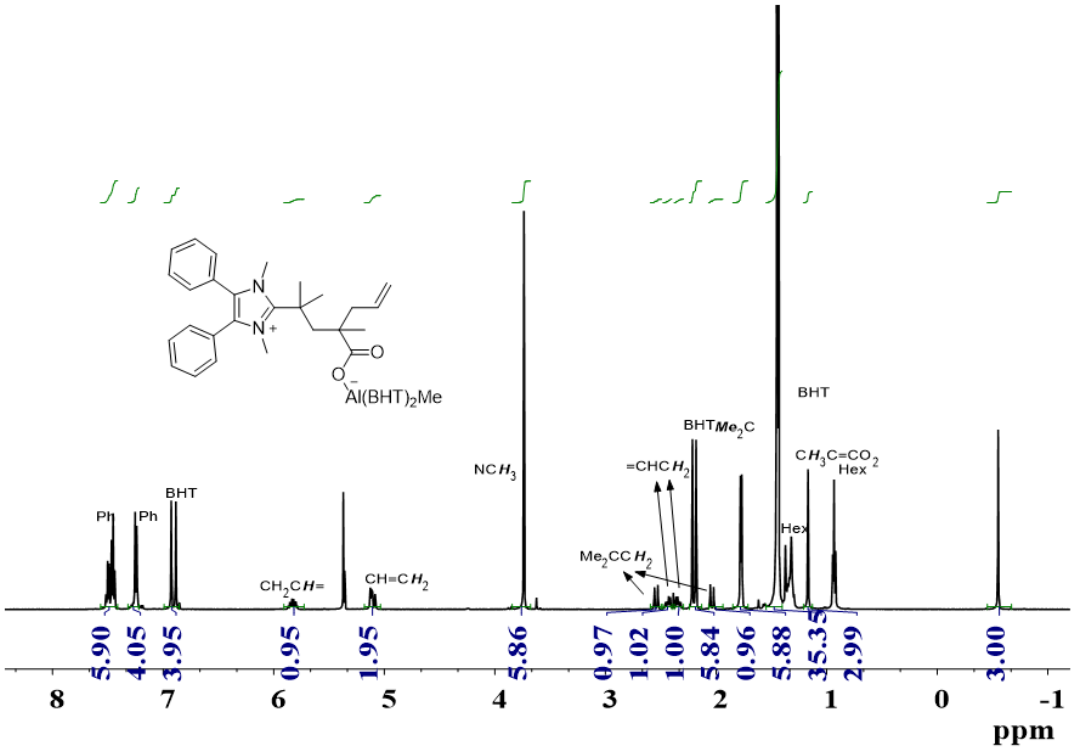

Fig S13 ^{1}H NMR spectrum (dichloromethane-d_2, 500 MHz) of **INT** isolated from the reaction **NHO1** with $MeAl(BHT)_2$·AMA = 1:1

6. Selected Polymerization Data

Table S1. NHO-catalyzed MMA polymerization[a]

Run	LB	M:LB:LA	Time	Conv.[b] (%)	M_n[c] (kg·mol^{-1})	$M_{n(calcd)}$ (kg·mol^{-1})	$Đ$ (M_w/M_n)	I*[d] (%)
1[e]	**NHO1**	800:1	24 h	72.8	68.4	58.6	2.86	86
2[e]	**NHO2**	800:1	24 h	85.3	87.3	68.6	2.82	79
3[e]	**NHO3**	800:1	24 h	48.3	63.5	38.8	1.25	61
4	**NHO4**	800:1	24 h	0	/	/	/	/
5	**NHO5**	800:1	24 h	0	/	/	/	/
6	**NHO6**	800:1	24 h	0	/	/	/	/
7	**NHO7**	800:1	24 h	0	/	/	/	/

[a] Condition: carried out at room temperature in 4.5 ml toluene, for a 200/2/1 MMA/LB/LA ratio, $[MMA]_0$ = 0.936 M, $[LA]_0 = 2[LB]_0$ = 9.36 mM. [b] Monomer conversions measured by ^{1}H NMR. [c] M_n and $Đ$ determined by GPC relative to PMMA standards in DMF. [d] Initiation efficiency (I*)% = M_n(calcd)/M_n(exptl) × 100, where M_n(calcd) = [MW(MMA)]([MMA]$_0$/[I]$_0$)(conversion)+MW of chain-end groups. [e] Data reported in our previous study (*ACS Catal.* **2018**, *8*, 3571−3578).

Table S2. Al(C_6F_5)$_3$-based LP-catalyzed MMA polymerization[a]

Run	LB	LA	M. (eq)	Time. min	Conv.[b] (%)	M_n[c] (kg·mol^{-1})	$Đ$ (M_w/M_n)	I*[d] (%)
1[e]	**NHO1**	Al(C_6F_5)$_3$	800	30 s	>99	85.9	1.07	94
2[e]	**NHO2**	Al(C_6F_5)$_3$	800	30 s	>99	80.6	1.05	100
3[e]	**NHO3**	Al(C_6F_5)$_3$	800	30 s	>99	88.6	1.03	91
4	**NHO4**	Al(C_6F_5)$_3$	200	30 s	>99	32.7	1.04	61
5	**NHO4**	Al(C_6F_5)$_3$	400	30 s	>99	55.7	1.03	72
6	**NHO4**	Al(C_6F_5)$_3$	800	1 min	>99	110	1.03	73
7	**NHO4**	Al(C_6F_5)$_3$	1600	2 min	>99	242	1.05	66
8	**NHO5**	Al(C_6F_5)$_3$	200	30 s	>99	31. 8	1.03	63
9	**NHO5**	Al(C_6F_5)$_3$	400	30 s	>99	58.3	1.02	69
10	**NHO5**	Al(C_6F_5)$_3$	800	30 s	>99	101	1.03	79
11	**NHO5**	Al(C_6F_5)$_3$	1600	3 min	>99	198	1.04	81
12	**NHO5**	Al(C_6F_5)$_3$	3200	17 min	>99	565	1.05	57
13	**NHO6**	Al(C_6F_5)$_3$	200	30 s	>99	29.2	1.04	69
14	**NHO6**	Al(C_6F_5)$_3$	400	30 s	>99	50.4	1.02	79
15	**NHO6**	Al(C_6F_5)$_3$	800	30 s	>99	97.3	1.03	82
16	**NHO6**	Al(C_6F_5)$_3$	1600	3 min	>99	198	1.04	81
17	**NHO6**	Al(C_6F_5)$_3$	3200	30 min	>99	459	1.06	70
18	**NHO7**	Al(C_6F_5)$_3$	800	3 min	>99	183	1.12	44

[a] Condition: carried out at room temperature in 4.5 ml toluene, for a 200/2/1 MMA/LB/LA ratio, $[MMA]_0$ = 0.936 M, $[LA]_0$ = 2$[LB]_0$ = 9.36 mM. [b] Monomer conversions measured by ^{1}H NMR. [c] M_n and $Đ$ determined by GPC relative to PMMA standards in DMF. [d] Initiation efficiency (I*)% = M_n(calcd)/M_n(exptl) × 100, where M_n(calcd) = [MW(MMA)]([MMA]$_0$/[I]$_0$)(conversion)+MW of chain-end groups. [e] Data reported in our previous study (*ACS Catal.* **2018**, *8*, 3571−3578).

7. MALDI-TOF MS Spectra of Low *MW* polymers by NHO based LPs

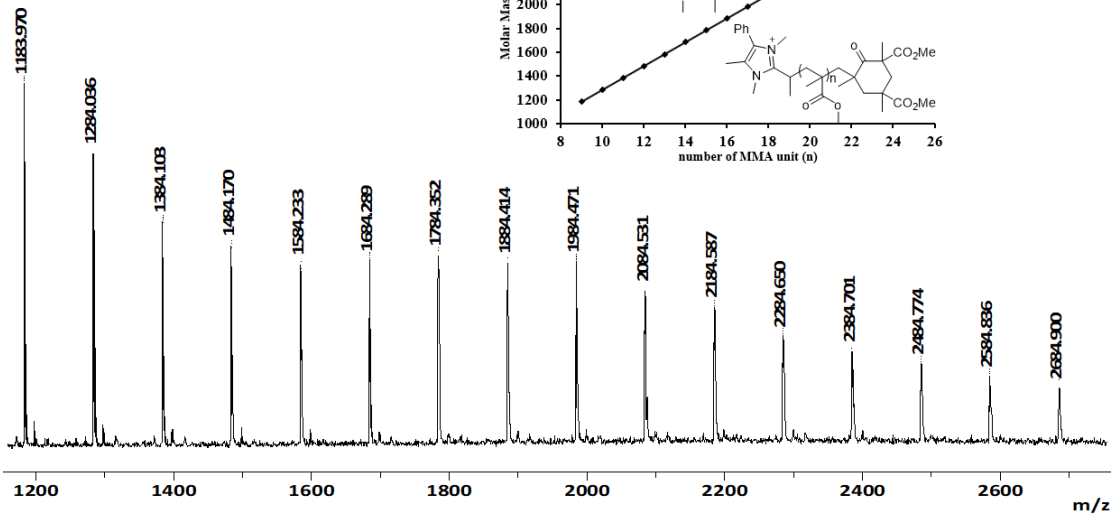

Fig S14. MALDI-TOF MS spectrum of the low-MW PMMA sample produced by **NHO5**/Al(C_6F_5)$_3$ in toluene at RT, and insert Fig: the number of MMA repeat units (*n*) and the deduced corresponding polymer chain structure.

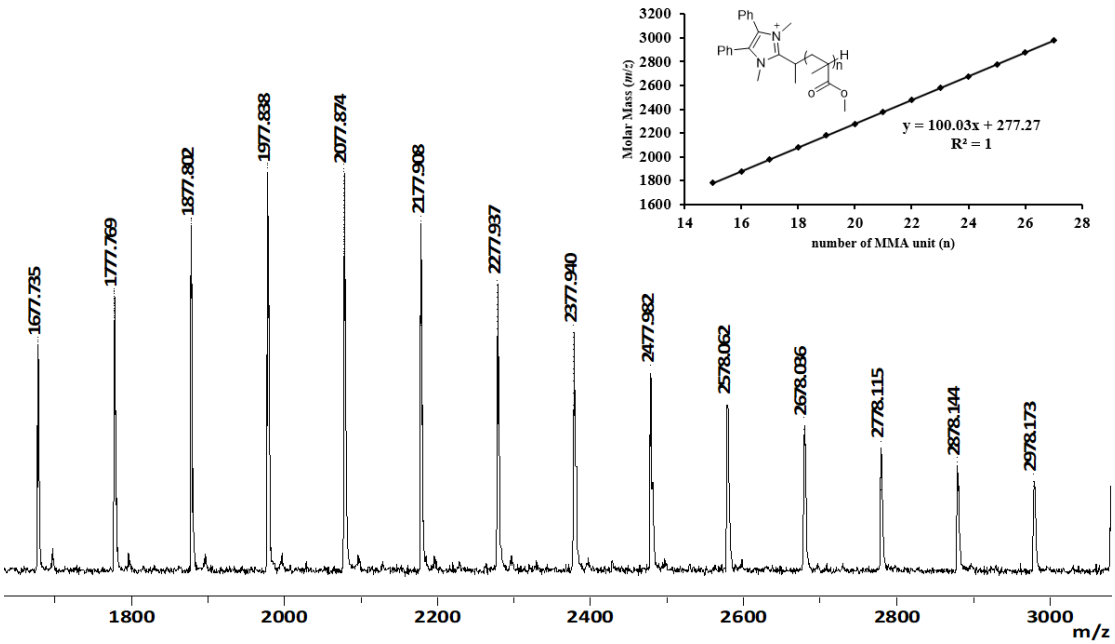

Fig S15. MALDI-TOF MS spectrum of the low-MW PMMA sample produced by **NHO4**/ MeAl(BHT)$_2$ in toluene at RT, and insert Fig: the number of MMA repeat units (*n*) and the deduced corresponding polymer chain structure.

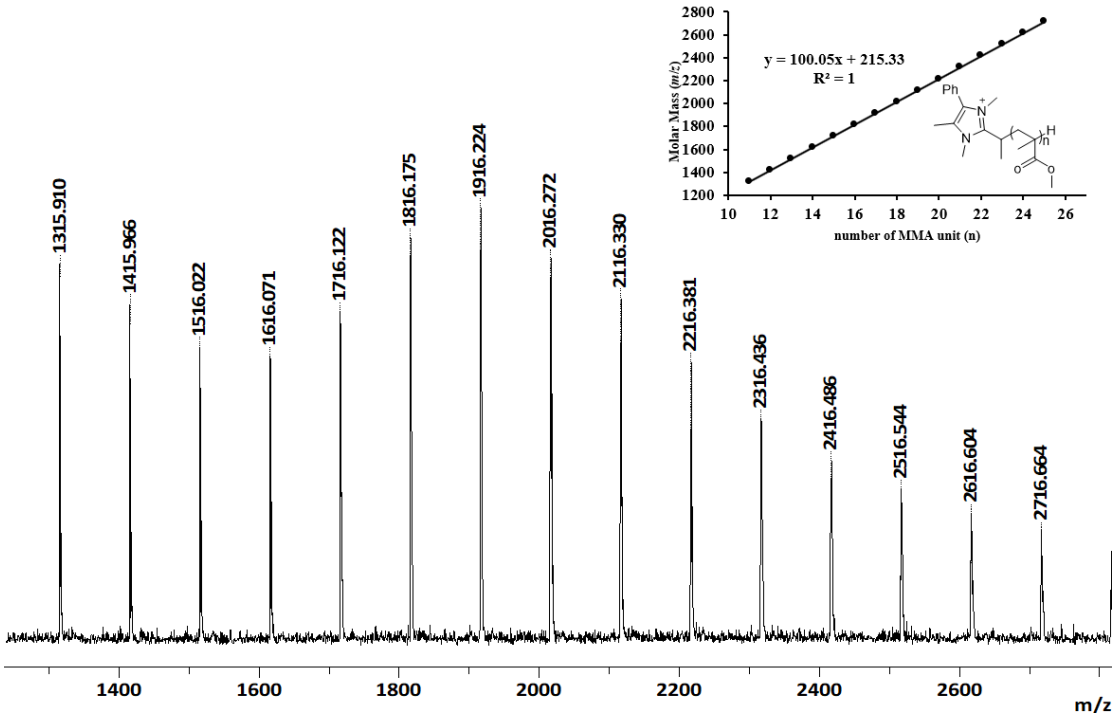

Fig S16. MALDI-TOF MS spectrum of the low-MW PMMA sample produced by **NHO5**/MeAl(BHT)$_2$ in toluene at RT, and insert Fig: the number of MMA repeat units (*n*) and the deduced corresponding polymer chain structure.

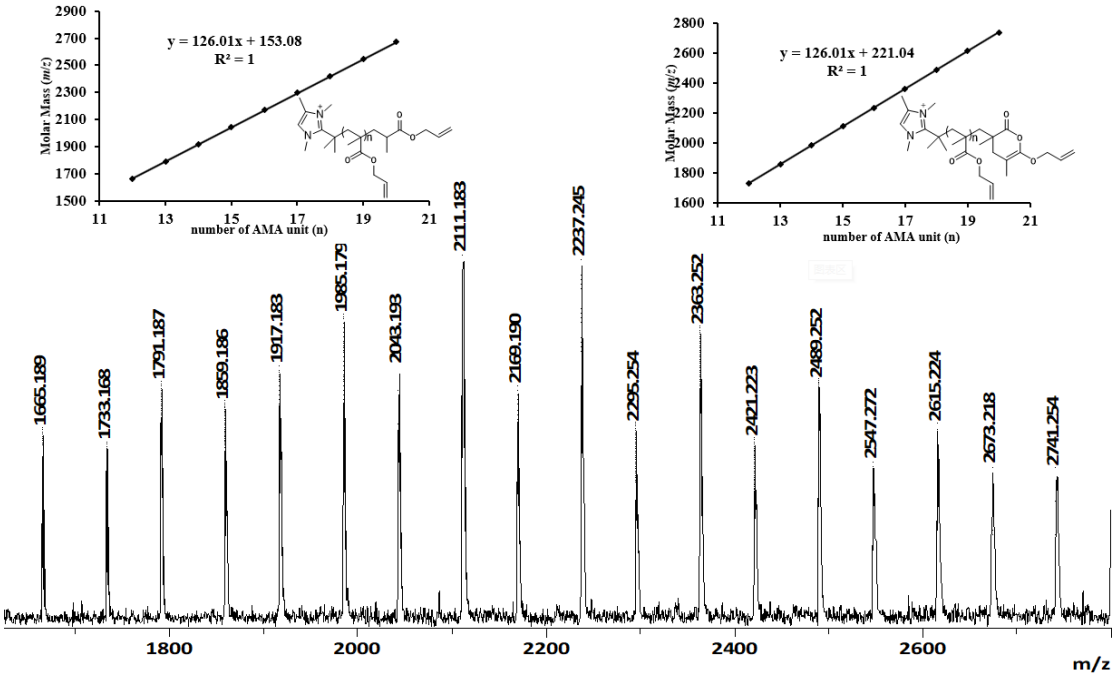

Fig S17. MALDI-TOF MS spectrum of the low-MW PAMA sample produced by **NHO3**/Al(C_6F_5)$_3$ in toluene at RT, and insert Fig: the number of AMA repeat units (*n*) and the deduced corresponding polymer chain structure.

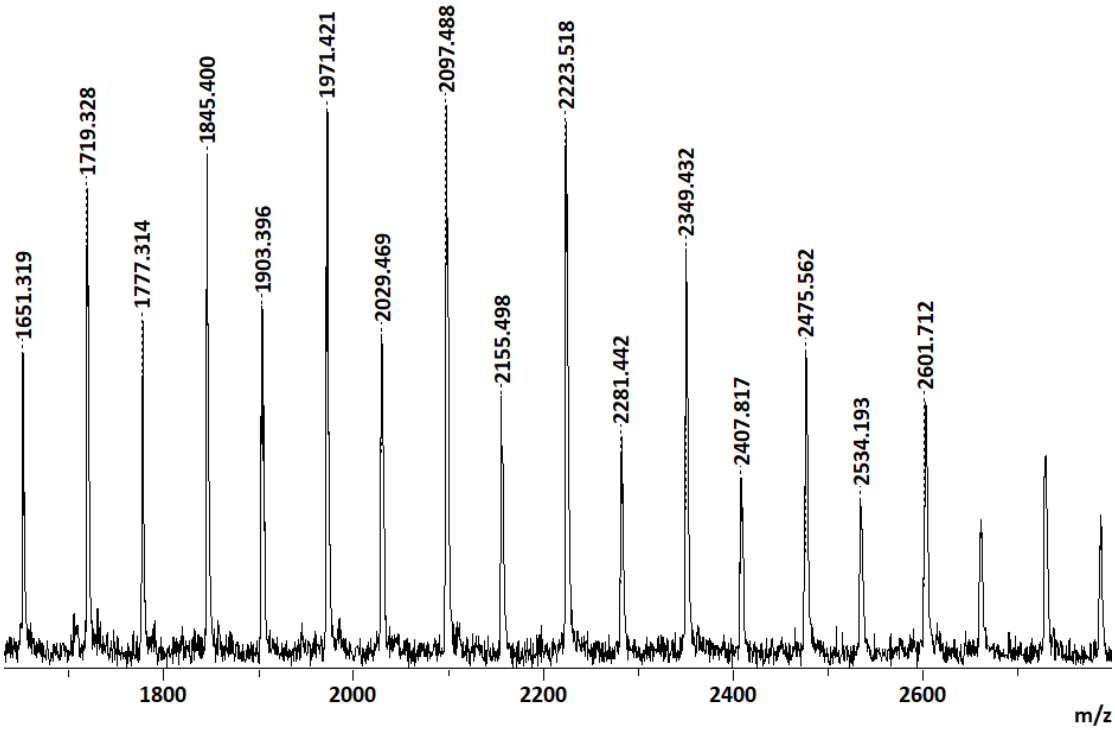

Fig S18. MALDI-TOF MS spectrum of the low-MW PAMA sample produced by **NHO6**/Al(C_6F_5)$_3$ in toluene at RT.

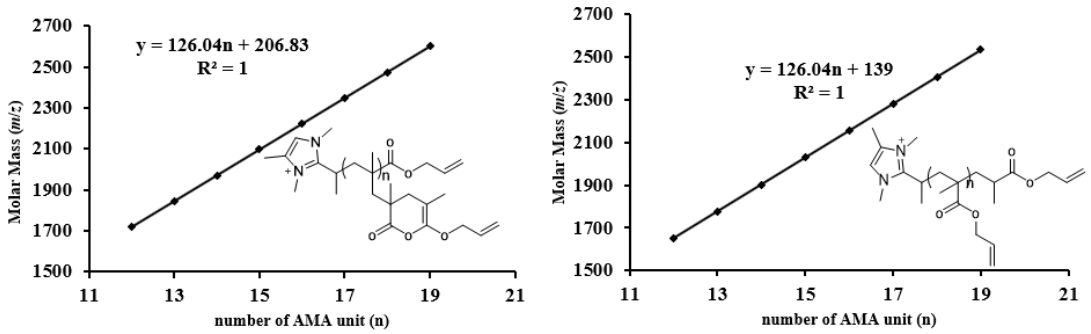

Fig S19. Plot of *m/z* values taken from Fig S18 vs the number of AMA repeat units (*n*) and the deduced corresponding polymer chain structures produced by **NHO3**/Al(C_6F_5)$_3$.

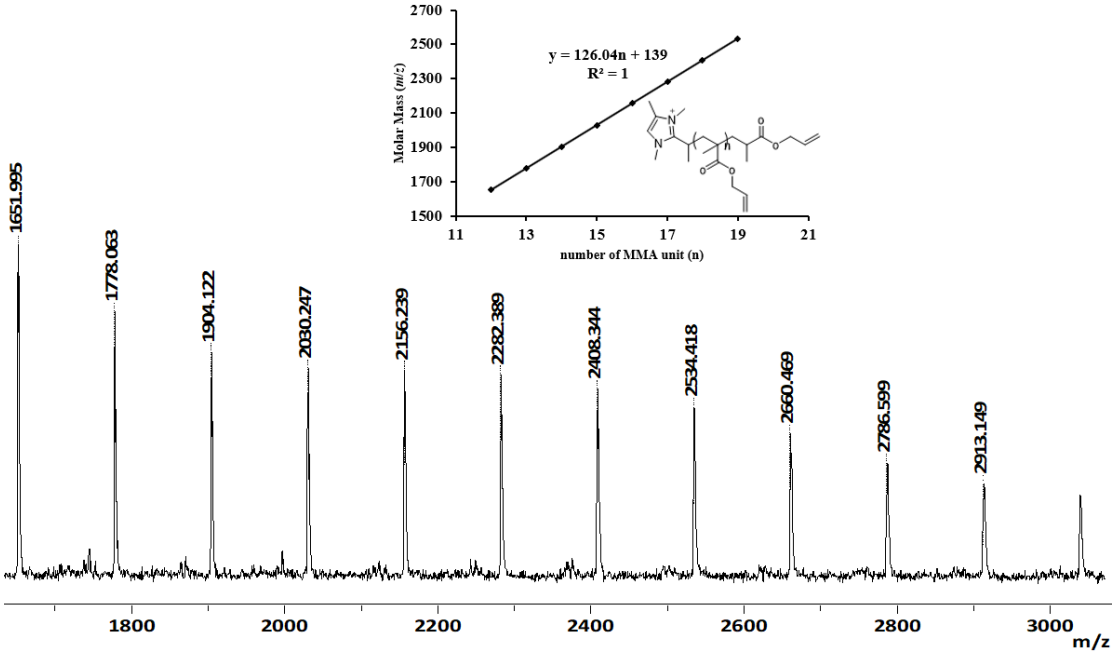

Fig S20. MALDI-TOF MS spectrum of the low-MW PAMA sample produced by **NHO6**/MeAl(BHT)$_2$ in toluene at RT, and insert Fig: the number of AMA repeat units (*n*) and the deduced corresponding polymer chain structure.

8. Chain Extension and copolymerization Experiments

Table S3. chain-extension and copolymerization polymerization by MeAl(BHT)$_2$/NHO[a]

Run	NHO	M1/M2/M3	Conv.[b] (%)	M_n[c] (kg·mol^{-1})	$Đ$
1	**NHO4**	400MMA	>99	45.8	1.06
2	**NHO4**	400/400MMA	>99	75.3	1.14
3	**NHO5**	400MMA	>99	48.9	1.06
4	**NHO5**	400/400MMA	>99	82.1	1.14
5	**NHO6**	400MMA	>99	40.8	1.07
6	**NHO6**	400/400MMA	>99	81.5	1.14
7[d]	**NHO1**	200MMA/200AMA (180s)/200MMA	MMA: > 99 AMA: > 99	66.1	1.16
8[e]	**NHO1**	200MMA /200AMA (240s)/200MMA	MMA: > 99 AMA: > 99	267 47.7(main)	1.11 1.09

[a] Condition: the first run was carried out with a 400/1/2 MMA/**NHO4**/MeAl(BHT)$_2$ ratio ([MMA]$_0$ = 0.936 M, [MeAl(BHT)$_2$]$_0$ = 2[**NHO4**]$_0$ = 4.68 mM) in 4.50 ml toluene at room temperature. [b] Monomer conversions measured by ^{1}H NMR. [c] M_n and $Đ$ determined by GPC relative to PMMA standards in DMF. [d] The GPC trace with a shoulder peak. [e] The GPC trace was bimodal distribution, a small peak appeared at higher molecular region.

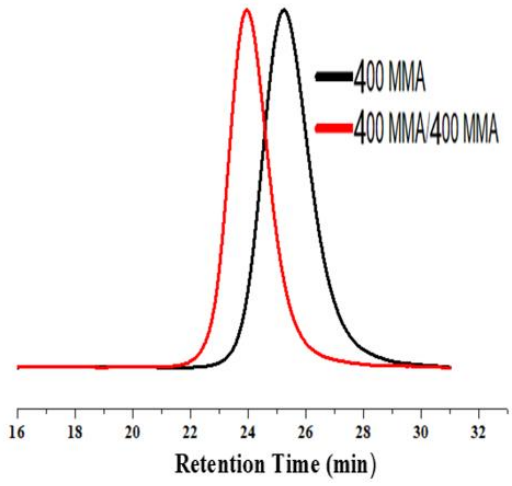

Fig S21. The GPC traces of PMMA samples obtained from chain extension experiments catalyzed by **NHO4**/MeAl(BHT)$_2$ in toluene at RT.

9. ^{1}H NMR spectrum of Polymers.

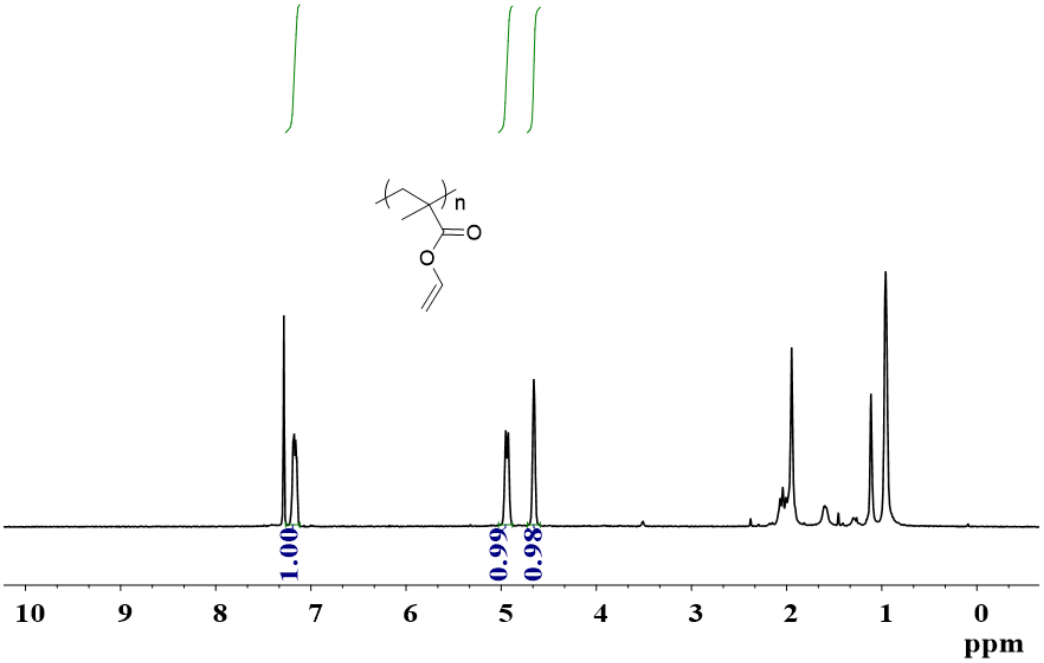

Fig S22. ^{1}H NMR spectrum (chloroform-*d*, 500 MHz) of PVMA.

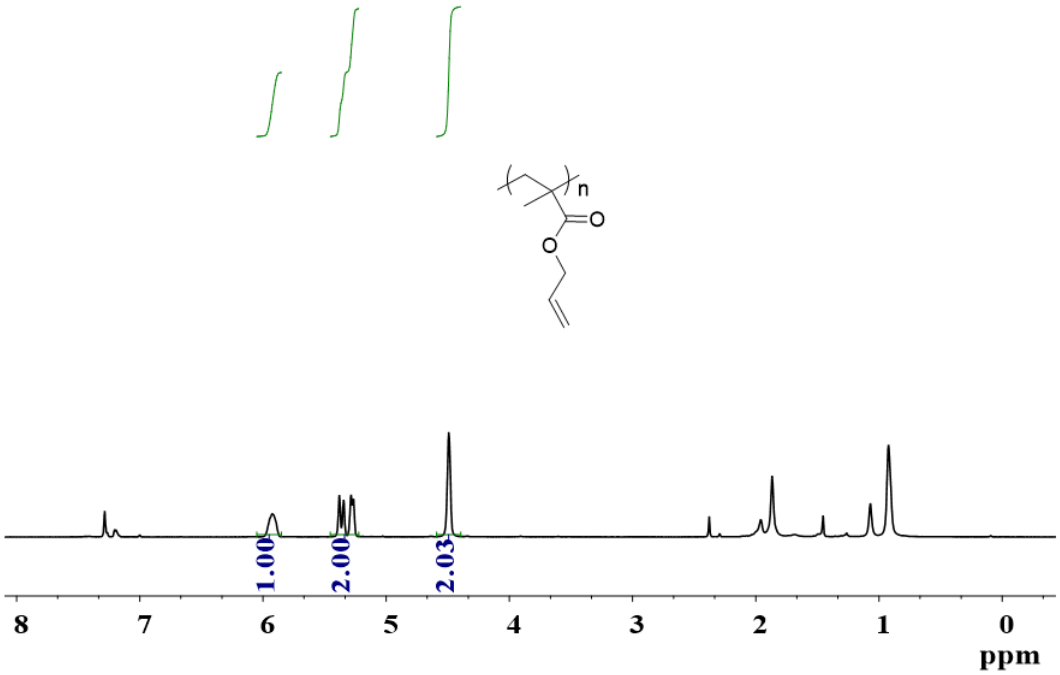

Fig S23. ^{1}H NMR spectrum (chloroform-*d*, 500 MHz) of PAMA.

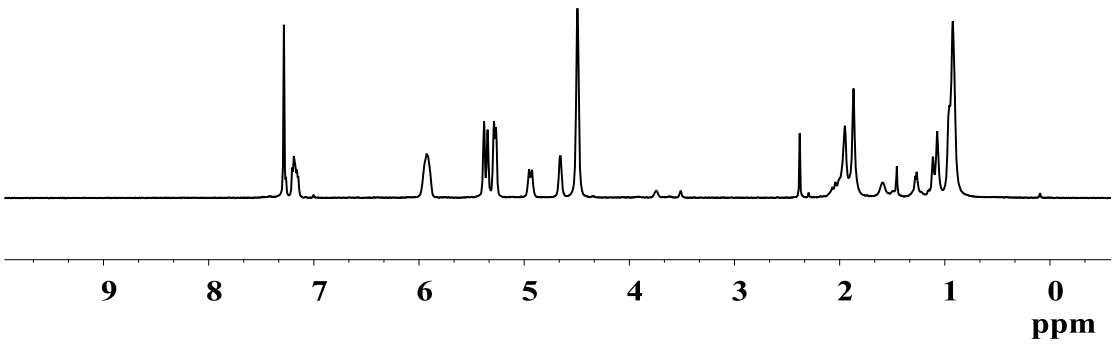

Fig S24. ^{1}H NMR spectrum (chloroform-*d*, 500 MHz) of PAMA-*b*-PVMA-*b*- PAMA.

10. Kinetics experiments

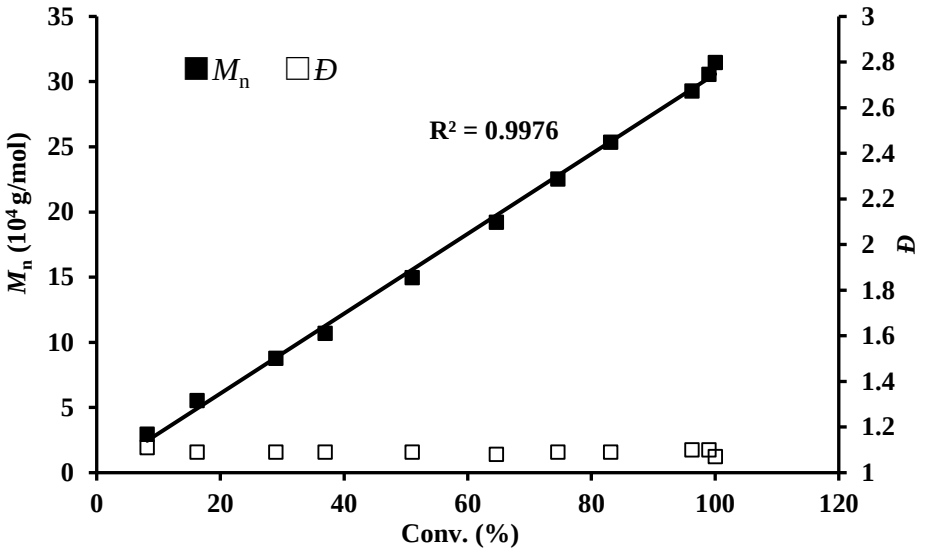

Fig S25. Plots of M_n and PDI of PMMA vs MMA conversion catalyzed by **NHO4**/MeAl(BHT)$_2$ at room temperature. Conditions: [MMA]/[**NHO4**]/[MeAl(BHT)$_2$] = 3200:1:2.

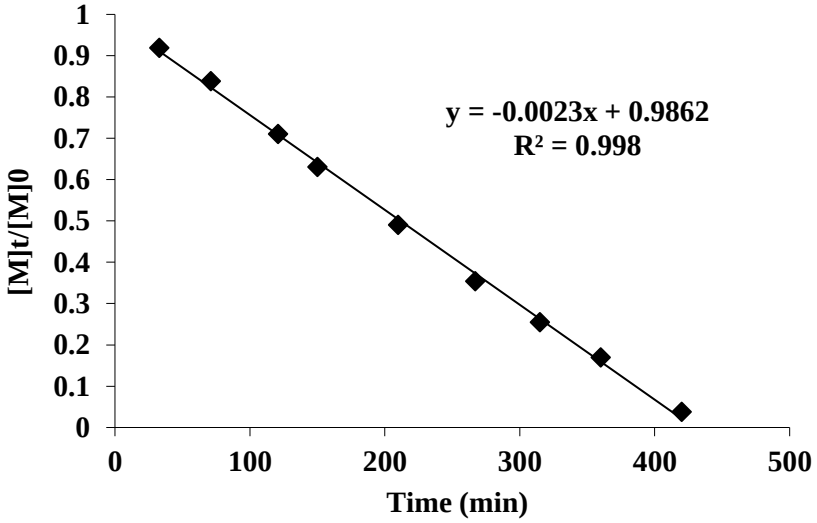

Fig S26 Zero-order kinetic plots for the MMA polymerization by **NHO4**/MeAl(BHT)$_2$ at room temperature. Comditions: [MMA]$_0$ = 0.936 M, [MMA]/[**NHO4**]/[MeAl(BHT)$_2$] = 3200:1:2.

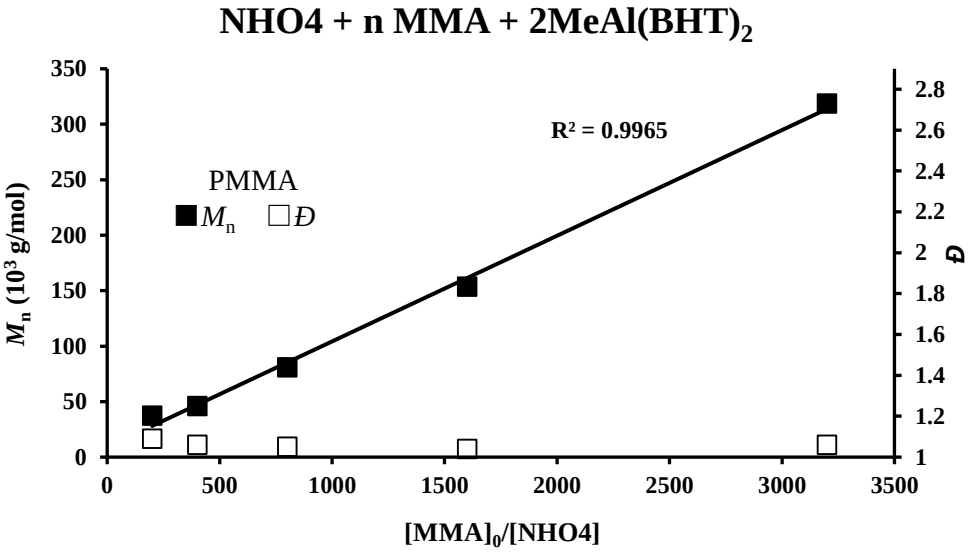

Fig S27. Plots of M_n and $Đ$ for PMMA vs $[MMA]_0/[$**NHO4**$]$ ratio.

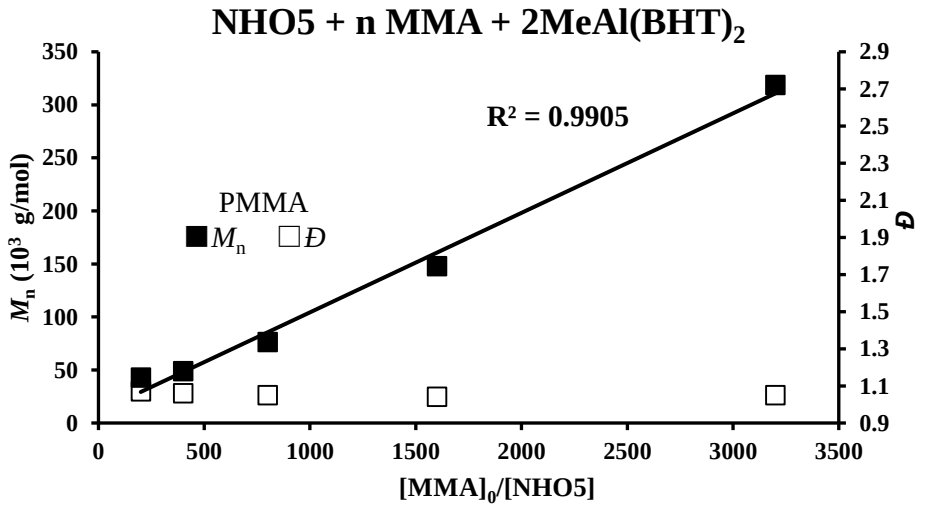

Fig S28. Plots of M_n and $Đ$ for PMMA vs $[MMA]_0/[$**NHO5**$]$ ratio.

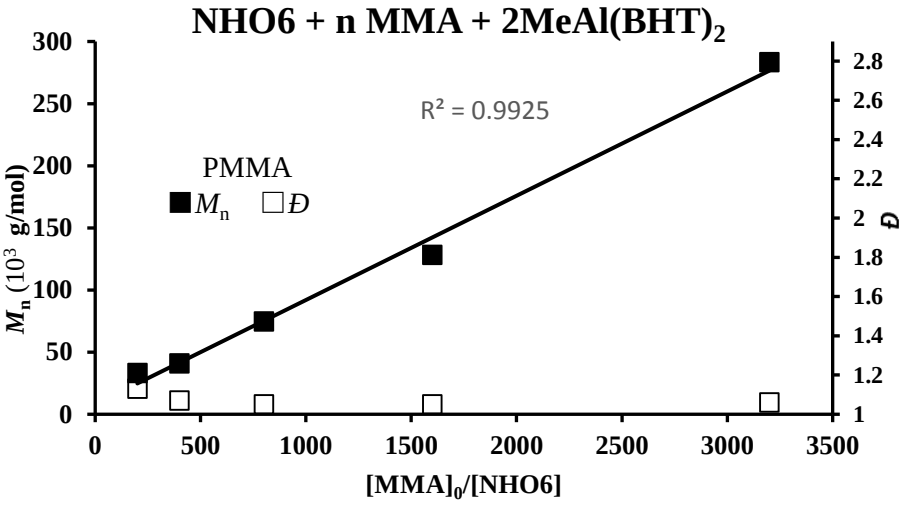

Fig S29. Plots of M_n and $Đ$ for PMMA vs $[MMA]_0/[$**NHO6**$]$ ratio.

11. References

(1) (a) Lehmann, M.; Schulz, A.; Villinger, A. Bissilylated Halonium Ions: $[Me_3Si{-}X{-}SiMe_3][B(C_6F_5)_4]$(X = F, Cl, Br, I). *Angew. Chem.; Int. Ed.* **2009**, *48*, 7444–7447. (b) Karsch, M.; Lund, H.; Schulz, A.; Villinger, A.; Voss, K. Molecular Networks Based on CN Coordination Bonds. *Eur. J. Inorg. Chem.* **2012**, *4*, 5542–5553.

(2) (a) Biagini, P.; Lugli, G.; Abis, L.; Andreussi, P. *U.S. Pat.* 5, 602269, **1997**. (b) C. H. Lee, S. J. Lee, J. W.; Park, K. H.; Kim, B. Y.; Lee, J. S. Oh, Preparation of $Al(C_6F_5)_3$ and its Use for the Modification of Methylalumoxane. *J. Mol. Cat., A: Chem.* **1998**, *132*, 231–239. c) Feng, S.; Roof, G. R.; Chen, E. Y.-X. Tantalum(V)-Based Metallocene, Half-Metallocene, and Non-Metallocene Complexes as Ethylene−1-Octene Copolymerization and Methyl Methacrylate Polymerization Catalysts. *Organometallics* **2002**, *21*, 832–839.

(3) Dong, J.; Chen, S.; Li, R.; Cui, W.; Jiang, H.; Ling, Y.; Yang, Z.; Hu, W. Imidazole-Based Pinanamine Derivatives: Discovery of Dual Inhibitors of the Wild-Type and Drug-Resistant Mutant of the Influenza A Virus. *Eur. J. Med. Chem.* **2016**, *108*, 605–615.

(4) E.; Gelens, De Kanter, F. J. J.; Schmitz, R. F.; Sliedregt, L. A. J. M.; Van Steen, B. J.; Kruse, C. G.; Leurs, R.; Groen, M. B.; Orru, R. V. A. Efficient Library Synthesis of Imidazoles Using a Multicomponent Reaction and Microwave Irradiation. *Mol. Diversity* **2006**, *10*, 17−22.

(5) Wang, Q.; Zhao, W.; He, J.; Zhang, Y.; Chen, E. Y.-X. Living Ring-Opening Polymerization of Lactones by *N*-Heterocyclic Olefin/$Al(C_6F_5)_3$ Lewis Pairs: Structures of Intermediates, Kinetics, and Mechanism. *Macromolecules* **2017**, *50*, 123−136.

(6) Stapleto, R. A.; Al-Humydi, A.; Chai, J.; Galan, B. R.; Collins, S. Sterically Hindered Aluminum Alkyls: Weakly Interacting Scavenging Agents of Use in Olefin Polymerization. *Organometallics* **2006**, *25*, 5083–5092.

(7) Wang, Q.; Zhao, W.; Zhang, S; He, J.; Zhang, Y.; Chen, E. Y.-X. Living Polymerization of Conjugated Polar Alkenes Catalyzed by N‑Heterocyclic Olefin-Based Frustrated Lewis Pairs. *ACS Catal.* **2018**, *8*, 3571−3578

(8) Joel E. Schmidt, Mark A. Deimund, Dan Xie, and Mark E. Davis. Synthesis of RTH-Type Zeolites Using a Diverse Library of Imidazolium Cations. *Chem. Mater.*, **2015**, *27*(10), 3756–3762